## Flux-Induced Vortex in Mesoscopic Superconducting Loops

Jorge Berger<sup>a</sup> and Jacob Rubinstein<sup>b</sup>

<sup>a</sup>Department of Physics, Technion, 32000 Haifa, Israel <sup>b</sup>Department of Mathematics, Technion, 32000 Haifa, Israel

We predict the existence of a quantum vortex for an unusual situation. We study the order parameter in doubly connected superconducting samples embedded in a uniform magnetic field. For samples with perfect cylindrical symmetry, the order parameter has been known for long and no vortices are present in the linear regime. However, if the sample is not symmetric, there exist ranges of the field for which the order parameter vanishes along a line, parallel to the field. In many respects, the behavior of this line is qualitatively different from that of the vortices encountered in type II superconductivity. For samples with mirror symmetry, this flux-induced vortex appears at the thin side for small fluxes and at the opposite side for large fluxes. We propose direct and indirect experimental methods which could test our predictions.

The question of where and under what conditions an individual vortex appears (or disappears) is still an active subject<sup>1-6</sup>. Here we consider an unusual setup: that of the Little-Parks experiment<sup>7-9</sup>, *i.e.* a superconducting loop which encloses a magnetic flux.

We find that, for a narrow range of enclosed fluxes in the vicinity of a half-integer number of quanta, a vortex is present in the loop. This vortex is completely different in nature from the traditional vortices known from type II superconductivity. In the traditional case, a minimum local magnetic field is required for the formation of a vortex; here, its formation is governed by the enclosed flux. As the magnetic field is increased, instead of having more and more vortices coming in, the present vortex disappears (and a new vortex appears only after an additional quantum of flux is enclosed by the loop). Whereas traditional vortices cannot exist along films which are thinner than the coherence length (they "need room for their cores")<sup>2</sup>, the present vortex exists for arbitrarily thin shells. Another atypical feature of the present vortex is its high anisotropy, which depends on the thickness of the shell. Moreover, there are cases in which the order parameter vanishes on a surface rather than a line.

Additional differences arise from the assumption that the total magnetic field remains equal to the applied field: whereas traditional vortices exist for type II superconductors, for which the Ginzburg-Landau parameter  $\kappa$  is larger than  $2^{-1/2}$ , the present vortex is insensitive to the London penetration depth and bears no connection with  $\kappa$ ; whereas traditional vortices cannot stay in equilibrium if the distance to the boundary is too short<sup>3</sup>, the equilibrium position of the present vortex is a continuous function of the flux and does reach the boundaries. This assumption is justified when either the thickness or the width of the loop is small compared to the magnetic penetration depth. The case in which the induced field is not negligible will be considered elsewhere.

We shall consider two complementary geometries: samples which almost have axial symmetry, which will be analyzed using perturbation, and samples with eccentric cylindrical boundaries, which will be studied by means of variation. In the first method the zeroth order configuration is a cylindrical shell of superconducting material, with inner radius R, outer radius R' = R + wand heigh h, where R, w and h are constants. In early experiments<sup>7</sup> h was much larger than R and w, whereas recent experiments<sup>8,9</sup> meet the opposite situation. We consider a uniform magnetic field parallel to the axis of the shell and study the onset of superconductivity. In this regime the magnetic field is still unaffected by the supercurrents and the Ginzburg-Landau equation is linearized to the eigenvalue problem

$$H_0\psi_0 = (i\nabla - 2\pi \mathbf{A}/\Phi_0)^2 \,\psi_0 = \psi_0/\xi_0^2 = E_0\psi_0.$$
(1)

 $\psi_0$  is the order parameter, **A** is the magnetic potential,  $\Phi_0$  is the quantum of fluxoid ( $\Phi_0 > 0$ ) and  $\xi_0$  is the coherence length at the onset of superconductivity. The notations for the function  $\psi_0$ , the operator  $H_0$  and the eigenvalue  $E_0$  have been introduced to remind of the eigenfunction, the Hamiltonian and the energy in a perturbation problem. Eq. (1) is subject to the condition that  $(i\nabla - 2\pi \mathbf{A}/\Phi_0)\psi$  has no normal component at the boundaries. (For the moment,  $\psi = \psi_0$ .) For a cylindrical shell and cylindrical coordinates  $(r, \theta, z)$ , Eq. (1) is separable and has been solved in [10]. Writing  $\psi_0 =$  $\mathcal{R}(r)\Theta(\theta)\mathcal{Z}(z)$ , one easily obtains  $\mathcal{Z}(z) = \cos(k\pi z/h)$ and  $\Theta(\theta) = e^{-mi\theta}$ , with k and m integers. Since  $E_0$ always increases with  $k^2$ , we pick k = 0 and the solution of Eq. (1) reduces to

$$\psi_0 = \mathcal{R}_m(r)e^{-mi\theta}.$$
 (2)

The winding number m is chosen so that lowest value of  $E_0$  is obtained. For a thin shell it is the closest integer to the number of flux quanta enclosed by the shell.  $\mathcal{R}_m$  was obtained in [10]; it depends on the magnetic field and involves a combination of Kummer functions, adjusted to meet the boundary conditions.

A salient feature of the solution (2) is that there exist magnetic fields for which Eq. (1) is degenerate. In the limit of a thin shell this occurs when the enclosed flux  $\Phi$ equals  $(m + \frac{1}{2})\Phi_0$ : for this flux, the eigenvalues  $E_0$  obtained for m and for m + 1 are the same and the lowest possible. If the shell is not thin, we can still define  $\Phi$  as the magnetic flux enclosed by the "representative circle"  $r = \bar{R} = R + w/2$ . There still exist fluxes  $\Phi_m^*$  (usually close to  $(m + \frac{1}{2})\Phi_0$ ) where the values of  $E_0$  for  $\psi_0 =$   $\mathcal{R}_m(r) \exp(-mi\theta)$  and for  $\psi_0 = \mathcal{R}_{m+1}(r) \exp(-[m+1]i\theta)$ coalesce. As the magnetic field is swept accross the situation  $\Phi = \Phi_m^*$ , the order parameter  $\psi_0$  changes discontinuously. With it, there is a jump in measurable quantities such as the current around the shell.

We perturb now the problem and consider a sample which is not a perfect cylindrical shell. To fix ideas, we still keep h and R constant, but take a nonuniform width

$$D(\theta) = w \left( 1 + \frac{\epsilon}{2} \sum_{j \neq 0} \beta_j e^{ji\theta} \right), \qquad (3)$$

where w is the average width,  $\epsilon \ll 1$  and  $\beta_{-j} = \beta_j$ . Other deviations from the perfect cylindrical problem lead to similar behavior.

The "Hamiltonian" is still  $H_0$ , but the eigenvalue and the eigenfunction are perturbed by the change in the boundary geometry. We write  $\psi = \psi_0 + \epsilon \psi_1 + \epsilon^2 \psi_2 + \ldots$ and  $E = E_0 + \epsilon E_1 + \epsilon^2 E_2 + \ldots$ , where  $\psi$  is the order parameter and  $E^{-1/2}$  the coherence length. The eigenvalue in our problem is related to the temperature T by

$$R^{2}E = (T_{c} - T)/(T_{c} - T_{R}), \qquad (4)$$

where  $T_c$  is the critical temperature in the absence of magnetic field and  $T_R$  the temperature at which the coherence length equals the internal radius R. The only reason for the requirement of a "mesoscopic" sample is to decrease  $T_R$  and thus widen the temperature scale  $T_c - T_R$ ; our formalism is valid for arbitrary positive R, w and h, and may cover the entire range from a very thin ring to an almost full disk. In order to decrease  $T_R$  we also require clean materials (usually type I), which have a large coherence length at zero temperature.

To proceed, we define a metric by integrating in the *unperturbed* region:  $(\phi_1, \phi_2) = \int_0^{2\pi} d\theta \int_R^{R'} r dr \bar{\phi}_1 \phi_2$ . It follows that

$$(\phi_1, H_0\phi_2) - (H_0\phi_1, \phi_2) = R' \int_0^{2\pi} \left(\phi_2 \frac{\partial \bar{\phi}_1}{\partial r} - \bar{\phi}_1 \frac{\partial \phi_2}{\partial r}\right) d\theta.$$
(5)

Far from  $\Phi_m^*$ , we obtain the sequence of equations  $(H_0 - E_0)\psi_1 = E_1\psi_0$ ,  $(H_0 - E_0)\psi_2 = E_1\psi_1 + E_2\psi_0$ , etc. The difference between this procedure and standard perturbation theory is that  $H_0$  is not Hermitian; instead, it obeys Eq. (5). To take this into account, we need  $\partial \psi_i / \partial r$ , evaluated at r = R'. To obtain this we expand  $\psi$  around r = R' and require to all orders of  $\epsilon$  that the normal current vanishes at  $r = R + D(\theta)$ . In this way we obtain that  $E_1 = 0$ ; the expressions for  $\psi_1$  and  $E_2$  are lengthy and will be reported elsewhere.

For  $\Phi \approx \Phi_m^*$ , the direct perturbation scheme described in the previous paragraph would lead to a divergent  $\psi_1$ . This divergence is due to the degeneracy at  $\Phi = \Phi_m^*$ . In this case we use degenerate perturbation theory, *i.e.* we write

$$\psi_0 = \mathcal{R}_m(r) \exp(-mi\theta) - \gamma \mathcal{R}_{m+1}(r) \exp(-[m+1]i\theta),$$
(6)

with the normalization  $\mathcal{R}_m(R) = \mathcal{R}_{m+1}(R) = 1$  and  $\gamma$ a coefficient which still has to be determined. Writing  $2\pi R^2 \mathbf{A} = \Phi_0[b_m + \epsilon \delta] r\hat{\theta}$ , with  $\bar{R}^2 b_m = \Phi_m^*/\Phi_0$ , and substituting into (5)  $\phi_1$  by  $\psi_0$  and  $\phi_2$  by  $\mathcal{R}_m(r) \exp(-mi\theta)$ or  $\mathcal{R}_{m+1}(r) \exp(-[m+1]i\theta)$ , leads to a system of equations for  $\gamma$  and  $E_1$ :

$$A_m\delta + B_m E_1 = C_m \beta_1 \gamma , \qquad (7)$$

$$A'_{m+1}\delta + B_{m+1}E_1 = C_m\bar{\beta}_1/\gamma , \qquad (8)$$

where

$$A_m = 2 \int_R^{R'} (mr - b_m r^3) \mathcal{R}_m^2 dr , \qquad (9)$$

$$A'_{m} = 2 \int_{R}^{n} (mr - b_{m-1}r^{3})\mathcal{R}_{m}^{2}dr , \qquad (10)$$

$$B_m = \int_R^R r \mathcal{R}_m^2 dr , \qquad (11)$$

$$C_m = \frac{1}{2} w R' \mathcal{R}_m(R') \mathcal{R}_{m+1}(R') \times [E_0 - (b_m R' - (m+1)/R')(b_m R' - m/R')] \quad (12)$$

and R has been taken as the unit of length. This system has two solutions and we choose the one with lower  $E_1$ . Note that this time  $E_1 \neq 0$ . After obtaining  $\psi_0$  and  $E_1$ ,  $\psi_1$  and  $E_2$  were also evaluated, but the details will be reported elsewhere.

The value of E provides the temperature at which the shell becomes superconducting. We have calculated it for a sample with a reasonable experimental shape:  $D(\theta) =$  $0.2R - 0.01R\cos(\theta)$ . The results are shown in Fig. 1. A customary approximation (e.g. [8]) for results in a thick shell is obtained by averaging the one-dimensional result for ideally thin shells. This procedure gives  $E_{\rm av} =$  $\int (\pi Br/\Phi_0 - m/r)^2 dr/w$ , where B is the magnetic field, m is the integer that minimizes this expression and the integral is from R to R'. A somewhat better approximation is obtained by taking  $\mathcal{R}_m$  constant (e.g. [9]). This gives  $E_{\rm const} = \int (\pi Br/\Phi_0 - m/r)^2 r dr / \int r dr$ .  $E_{\rm const}$  is also shown in Fig. 1 for comparison. We see that  $E_{\text{const}}$ is quite a good approximation, but it exhibits cusps when the value of m changes, whereas for our treatment E is smooth. This qualitative difference does not arise from the dependence of  $\mathcal{R}_m$  on r; what happens is that the superposition of two values of m produces a sinusoidal dependence of  $|\psi|^2$  on  $\theta$ .<sup>11</sup> The size and the extent of the decline of  $T_c - T$  near  $\Phi_m^*$  are proportional to  $\epsilon \beta_1$ , which measures the deviation from a uniform shell.

In Fig. 2 we show contour plots of  $|\psi|$  in a narrow radial strip next to  $\theta = 0$  for six equidistant fluxes between  $\Phi = 0.501364\Phi_0$  and  $\Phi = 0.501382\Phi_0$ .  $\Phi_0^* = 0.501376\Phi_0$ is contained in this range. We have chosen an example with the width D symmetric about  $\theta = 0$  and  $\theta = \pi$ , so that the plots can be continued by placing a mirror at  $\theta =$ 0. As  $\Phi$  increases and comes close to  $\Phi_0^*$ ,  $|\psi|$  decreases at the axial line  $(r = R + D(0), \theta = 0)$ , until in frame (b)  $\psi(R + D(0), 0) = 0$ : this is the field at which the vortex appears. As the flux is increased further, the equilibrium position of the vortex moves towards the inner boundary, which is reached in frame (e). If the field is increased further, the vortex disappears. The extent of the flux range for which the vortex exists is proportional to  $\epsilon\beta_1$ .

In the general case the vortex is located at  $\theta = \arg(-C_m\bar{\beta}_1)$ ; if *m* is small and *D* is symmetric, as in the example we picked, this corresponds to the thinnest part of the shell. For large values of  $m \ (m \ge 5 \text{ for } w = 0.2R)$ ,  $C_m$  becomes negative and the vortex is located at the opposite side of the shell.

Knowing  $\psi(r,\theta)$ , we can evaluate the supercurrent. Fig. 3 shows the streamlines for the same fluxes considered in Fig. 2. Each frame shows 1/20 of the shell, with the plane  $\theta = 0$  at the left.

The perturbational approach is theoretically instructive, but since the range of existence of the vortices increases with nonuniformity, we are interested in sample shapes that are very far from axial symmetry. We conjecture that the scenario found above is generic for samples that are not symmetric. To support this conjecture, we consider a sample with cylindrical boundaries. The inner (outer) radius will again be denoted by R(R'), but the axes of both boundaries do not coalesce.  $\Phi$  will still be the flux through a circle of radius  $\bar{R} = \frac{1}{2}(R+R')$ . It is natural to use bipolar coordinates,<sup>12</sup>  $x + iy = c \tanh[(\alpha + i\beta)/2]$ , where x and y are the Cartesian coordinates perpendicular to the axes and ca constant which defines the lengthscale. The lines of constant  $\alpha$  are circles; we assign  $\alpha_1 = \operatorname{arcsinh}(c/R')$ ,  $\alpha_2 = \operatorname{arcsinh}(c/R)$ , and the sample occupies the region  $\alpha_1 \leq \alpha \leq \alpha_2, -\pi \leq \beta \leq \pi$ . Thinner samples (smaller (R' - R)/R) are obtained by taking small differences  $\alpha_2 - \alpha_1$ , whereas more eccentric samples (larger  $D(\pi)/D(0)$  are obtained by taking both  $\alpha_1$  and  $\alpha_2$  small. The shape shown in Fig. 4 corresponds to  $\alpha_1 = 0.5$ ,  $\alpha_2 = 0.7.$ 

The magnetic potential can be written in the form

$$\mathbf{A} = \frac{\Phi(\cosh\alpha + \cos\beta)}{\pi c \bar{R}^2} \left[ f(\alpha, \beta) - f(\bar{\alpha}, \beta) - \frac{\bar{R}^2}{2} \right] \hat{\beta},$$
  
$$f(\alpha, \beta) = c^2 \sin^{-2}\beta \left[ \sinh\alpha/(\cosh\alpha + \cos\beta) - 2 \arctan(\tan\frac{\beta}{2} \tanh\frac{\alpha}{2}) \cot\beta \right],$$
(13)

with  $\bar{\alpha} = \operatorname{arcsinh}(c/\bar{R})$ .

An approximation for the order parameter  $\psi$  will be obtained by means of a variational procedure.<sup>13</sup> The eigenvalue and the eigenvector for the onset of superconductivity may be obtained by minimizing the ratio  $\int |(i\nabla - 2\pi \mathbf{A}/\Phi_0)\psi|^2 dV / \int |\psi|^2 dV$ , where dV is the element of volume and the integrals are over the sample. Using the boundary conditions,  $\psi$  can be written as a Fourier series

$$\psi = \sum_{m=-\infty}^{\infty} \sum_{l=0}^{\infty} \left( c_{ml} \cos\left(l\pi \frac{2\alpha - \alpha_2 - \alpha_1}{\alpha_2 - \alpha_1}\right) + s_{ml} \sin\left(\frac{(2l+1)\pi}{2} \frac{2\alpha - \alpha_2 - \alpha_1}{\alpha_2 - \alpha_1}\right) \right) e^{mi\beta}.$$
 (14)

 $(\psi$  is again independent of z.) We truncate now this series and leave only a finite set of nonzero coefficients. The number of terms which is required to achieve some desired accuracy increases with  $\Phi$  and with (R'-R)/R, while it is not very sensitive to eccentricity. In our calculations we have kept eight coefficients:  $c_{m_0-2,0}$ ,  $c_{m_0-1,0}$ ,  $c_{m_0,0}$ ,  $c_{m_0+1,0}$ ,  $c_{m_0+2,0}$ ,  $s_{m_0-1,0}$ ,  $s_{m_0,0}$ ,  $s_{m_0+1,0}$ , where the integer  $m_0$  is chosen to obtain the minimum eigenvalue.

Regarding these coefficients as a vector

$$\mathbf{v} = \{c_{m_0-2,0}, c_{m_0-1,0}, c_{m_0,0}, c_{m_0+1,0}, \\ c_{m_0+2,0}, s_{m_0-1,0}, s_{m_0,0}, s_{m_0+1,0}\},\$$

we can write  $\int |(i\nabla - 2\pi \mathbf{A}/\Phi_0)\psi|^2 dV = \mathbf{v}^{\dagger}\mathbf{M}\mathbf{v}$  and  $\int |\psi|^2 dV = \mathbf{v}^{\dagger}\mathbf{Q}\mathbf{v}$ , where the elements of the matrices  $\mathbf{M}$  and  $\mathbf{Q}$  are easily evaluated. We are therefore left with the minimization of the ratio  $(\mathbf{v}^{\dagger}\mathbf{M}\mathbf{v})/(\mathbf{v}^{\dagger}\mathbf{Q}\mathbf{v})$ . This ratio is minimized for the eigenvector of  $\mathbf{Q}^{-1}\mathbf{M}$  that has the lowest eigenvalue. The error introduced by truncation may be estimated by the size of the discontinuity of  $\psi$  at the values of  $\Phi$  for which  $m_0$  changes.

Using this method, we rediscover the behavior obtained for almost axially symmetric samples: near halfinteger fluxes, a vortex appears at the outer boundary and moves towards the inner boundary as the flux is increased. What looks more striking, is that again these vortices enter through the thin side for small numbers of quanta and through the opposite side when  $\Phi/\Phi_0$  is sufficiently large. If  $\alpha_{1,2}$  are chosen to reproduce the shape used in our previous perturbation example, the length of the range for which the vortex is present agrees to about  $10^{-8}\Phi_0$  with the result obtained by perturbation. The values of the flux for which the vortex appears agree to about  $10^{-6}\Phi_0$  in both methods. Fig. 4 shows contour plots of  $|\psi|$  for  $\alpha_1 = 0.5$ ,  $\alpha_2 = 0.7$  and for fluxes chosen so that the vortex is approximately midway between the inner and the outer boundary. For these values of  $\alpha_{1,2}$ and for  $\Phi \leq 5\Phi_0$ , we estimate the error in  $\psi$  to be a few percent of the maximum value of  $|\psi|$ .

In conclusion, we have found a setup for which a new kind of vortex exists. Its existence is governed by the flux enclosed in the entire shell rather than by the local magnetic field. Likewise, the position of the vortex is a function of the entire sample (and of the flux) rather than of local defects. The ocurrence of this vortex is a nearly periodic function of the flux. The presence of a vortex implies that the flux lies within a very narrow known range.

It should be stated, however, that the magnetic field in the superconducting material itself does influence the nature of these vortices. For instance, we have found that if the field is constant in the region  $0 \le r \le \overline{R}$  and has opposite sign outside this region, then, as  $\Phi$  increases close to  $\Phi_m^*$ , a vortex and an antivortex form at a point somewhere in the middle of the shell; as the flux increases further, the vortex moves from this point towards the inner boundary and the antivortex towards the outer boundary, until they disappear. Moreover, if the field vanishes in the entire shell, then the vortex becomes a cut,<sup>14</sup> *i.e.* the order parameter vanishes on a surface that connects the inner and the outer boundaries.

Finally, we discuss the experimental possibilities for the detection of the vortex predicted here. We require a sample such that its size is of the order of the coherence length for a reasonable range of temperatures. Typical experiments for this purpose use samples made of Al, with a perimeter of a few  $\mu$ m. In order to observe the vortices directly, we require an imaging technique with spatial resolution of the order of 0.1  $\mu$ m. This requirement is met by scanning tunneling microscopy,<sup>15</sup> magnetic decoration<sup>16</sup> and electron holography.<sup>17</sup> When interpreting electron holography it should be born in mind that for the vortex predicted here only the fluxoid equals  $\Phi_0$ ; its magnetic flux alone will be much smaller and temperature dependent. Clearly, in order to sense the local density of states or the current density, the size of the order parameter must be above some threshold required by the sensitivity of the experiment. In this regime Eq. (1)for the onset of superconductivity becomes insufficient and we have to analyze the nonlinear Ginzburg-Landau equations. We have partially analyzed this situation and anticipate here some results. The existence and behavior of the vortex remain qualitatively the same as reported here for some temperature range below the onset of superconductivity. This temperature range increases with the deviation from a uniform shell.

Direct observation of the vortex is expected to be a difficult experiment, since the requirement of large coherence lengths implies a small gap. In addition, evaporated Al usually has a rough surface. Therefore, it might be helpful to obtain indirect evidence for the scenario encountered here. In the limit of thin shells, we know that there exist critical points at fluxes close to  $\Phi_m^*$  and at some temperature which we denote  $T_2^{(m)}$ . Below  $T_2^{(m)}$  the current I around the loop exhibits hysteresis, whereas above  $T_2^{(m)}$  it is reversible and continuous. Moreover, above and near  $T_2^{(m)}$ ,  $dI/d\Phi$  has a maximum near  $\Phi = \Phi_m^*$ , which diverges as  $T_2^{(m)}$  is approached.<sup>18</sup> Our analysis of the nonlinear Ginzburg-Landau equations shows that these features remain valid when the shell is thick. In particular, the divergence of  $dI/d\Phi$  at the critical point is not smeared.

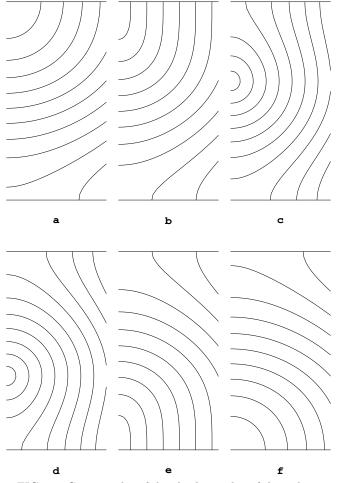
We therefore need a technique that measures  $dI/d\Phi$ , which is proportional to the ac magnetic susceptibility. This is measured by applying a bias flux with a superimposed small ac signal. The response is the ac component of the induced magnetic flux in some region. This induced flux has already been measured by means of a SQUID microsusceptometer.<sup>9</sup> Other techniques which seem appropriate for this measurement are the piezoresistive cantilever<sup>19</sup> and the ballistic Hall magnetometer.<sup>20</sup> The Hall magnetometer seems particularly promising, because, if only part of the sample is located on the active region of the probe, it would allow to measure the flux induced at that part.

This research was supported by the US-Israel Binational Science Foundation and by the Israel Science Foundation. We thank A. Auerbach, Y. Eckstein, B. Fisher and V. Kogan for useful suggestions. We thank V. Bruyndoncx, V. Moshchalkov, B. Pannetier and C. Van Haesendonck for clarifying to us some of the experimental possibilities and limitations.

- <sup>1</sup> A. A. Abrikosov, Sov. Phys. JETP **19**, 988 (1964); L. Kramer, Phys. Lett. A **24**, 571 (1967); L. G. Aslamazov and A. I. Larkin, JETP Lett. **9**, 87 (1969); V. V. Shmidt, Sov. Phys. JETP **30**, 1137 (1970); K. K. Likharev, Sov. Phys. JETP **34**, 906 (1972).
- <sup>2</sup> R. D. Parks, J. M. Mochel and L. V. Surgent, Phys. Rev. Lett. **13**, 331 (1964); M. Tinkham, *Introduction to Super*conductivity (McGraw-Hill, N.Y., 1996).
- <sup>3</sup> C. P. Bean and J. D. Livingston, Phys. Rev. Lett. **12**, 14 (1964); J. Rubinstein, Zeit. Angew. Math. Phys. **46**, 739 (1995).
- <sup>4</sup> T. Yamashita and L. Rinderer, J. Low Temp. Phys. **24**, 695 (1976); H. Frahm, S. Ullah and A. T. Dorsey, Phys. Rev. Lett. **66**, 3067 (1991); F. Liu, M. Mondello and N. Goldenfeld, Phys. Rev. Lett. **66**, 3071 (1991); S. H. Brongersma *et al.*, Phys. Rev. Lett. **71**, 2319 (1993); M. Machida and H. Kaburaki, Phys. Rev. Lett. **71**, 3206 (1993); R. Kato, Y. Enomoto and S. Maekawa, Phys. Rev. B **47**, 8016 (1993); G. Stejic *et al.*, Phys. Rev. B **49**, 1274 (1994); A. Gurevich and L. D. Cooley, Phys. Rev. B **50**, 13 563 (1994); P. Lobotka *et al.*, Physica C **229**, 231 (1994); C. Bolech, G. Buscaglia and A. López, Phys. Rev. B **52**, R15 719 (1995).
- <sup>5</sup> D. Saint-James, G. Sarma and E. J. Thomas, *Type II superconductivity* (Pergamon, Oxford, 1969); W. H. Zurek, Phys. Rep. **276**, 177 (1996); G. W. Crabtree and D. R. Nelson, Physics Today, April 1997, p. 38.
- <sup>6</sup> K. W. Schwarz, Phys. Rev. Lett. **64**, 1130 (1990); R. J. Donnelly, *Quantized Vortices in Helium II* (Cambridge Univ. Press, Cambridge,1991); T. Frisch, Y. Pomeau and S. Rica, Phys. Rev. Lett. **69**, 1644 (1992); Y. Pomeau and S. Rica, Phys. Rev. Lett. **71**, 247 (1993); U. C. Täuber and D. R. Nelson, Phys. Rep. **289**, 157 (1997).
- <sup>7</sup> W. A. Little and R. D. Parks, Phys. Rev. Lett. 9, 9 (1962); R. P. Groff and R. D. Parks, Phys. Rev. 176, 567 (1968).
- <sup>8</sup> V. V. Moshchalkov *et al.*, Nature **373**, 319 (1995).
- <sup>9</sup> X. Zhang and J. C. Price, Phys. Rev. B **55**, 3128 (1997).
- <sup>10</sup> R. B. Dingle, Proc. R. Soc. London, Ser. A **211**, 500 (1952);
   D. Saint-James, Phys. Lett. **15**, 13 (1965); R. Benoist and
   W. Zwerger, Z. Phys. B103, 377 (1997); V. V. Moshchalkov,
   X. G. Qiu and V. Bruyndoncx, Phys. Rev. B **55**, 11 793 (1997).
- <sup>11</sup> J. Berger and J. Rubinstein, SIAM J. Appl. Math. 58, 103 (1998).
- <sup>12</sup> P. M. Morse and H. Feshbach, Methods of Theoretical Physics (McGraw-Hill, N.Y., 1953); N. N. Lebedev, I. P. Skalskaya and Y. S. Uflyand, Worked Problems in Applied Mathematics (Dover, N. Y., 1965).
- <sup>13</sup> S. H. Gould, Variational Methods for Eigenvalue Problems (University of Toronto, Toronto, 1966); De Gennes P.-G., Superconductivity of Metals and Alloys (Addison-Wesley, reading, 1989); V. M. Fomin, J. T. Devreese and V. V. Moshchalkov, Europhys. Lett. **42**, 553 (1998); J. J. Palacios, Phys. Rev. B **57**, 10873 (1998).
- <sup>14</sup> J. Berger, J. Rubinstein and M. Schatzman in *Proceedings* of the International Conference on Calculus of Variations, A. Ioffe et al. Eds., CRC Press, in press.
- <sup>15</sup> A. L. Lozanne, S. A. Elrod and C. F. Quate, Phys. Rev.

Lett. 54, 2433 (1985); H. F. Hess *et al.*, Phys. Rev. Lett.
62, 214 (1989); Ch. Renner *et al.*, Phys. Rev. Lett. 67, 1650 (1991).

- <sup>16</sup> H. Träuble and U. Essmann, J. Appl. Phys. 25, 273 (1968);
   P. L. Gammel *et al.*, Phys. Rev. Lett. 59, 2592 (1987).
- <sup>17</sup> T. Matsuda *et al.*, Phys. Rev. Lett. **62**, 2519 (1989); J.
   E. Bonevich *et al.*, Phys. Rev. Lett. **70**, 2952 (1993); A.
   Tonomura, *Electron Holography* (Springer, Berlin, 1993).
- <sup>18</sup> J. Berger and J. Rubinstein, Phys. Rev. B **56**, 5124 (1997).
- <sup>19</sup> A. Volodin and C. Van Haesendonck, Appl. Phys. A 66, S305 (1998).
- <sup>20</sup> A. K. Geim, I. V. Grigorieva, S. V. Dubonos, J. G. S. Lok, J. C. Maan, A. E. Filippov, and F. M. Peeters, Nature **390**, 259 (1997).



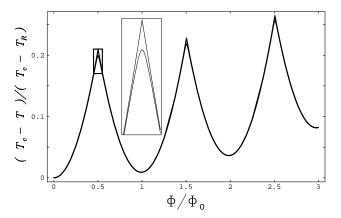
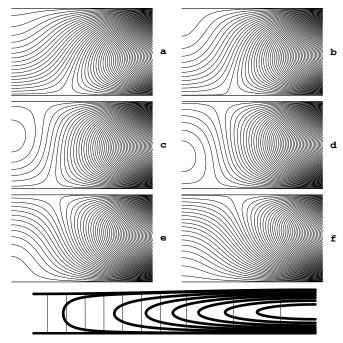


FIG. 1. Temperature T for the onset of superconductivity as a function of the magnetic flux  $\Phi$  enclosed by the "representative" circle. The graph shows two curves, which nearly coincide. The lower curve corresponds to the formalism developed here; for comparison,  $E_{\rm const}$  (see text) has also been drawn. The inset shows an enlarged view of the region enclosed by the rectangle. The lower curve in the inset looks smooth, but was calculated using three different algorithms in different regions: m = 0, degenerate perturbation and m = 1; likewise, near  $\Phi = \Phi_1^* \approx 1.5\Phi_0$ , m = 1, degenerate perturbation and m = 2 match smoothly, and so on.

FIG. 2. Contour plot of the absolute value of the order parameter in a narrow radial slice of the superconducting shell, for increasing values of the magnetic field. The horizontal coordinate is  $|\theta|$ , in the region  $0 \le |\theta| \le 0.0002\pi$ ; the vertical coordinate is  $R \le r \le 1.19R$ . The plane  $\theta = 0$  is located at the left of each frame. In (a),  $|\psi|$  has a minimum at the line  $(r = 1.19R, \theta = 0)$ . In (b),  $\psi$  vanishes along this line in the outer boundary and the vortex appears. As the magnetic field increases, the vortex shifts towards the inner boundary r = R and reaches it in (e). In (f),  $|\psi| > 0$  everywhere and the vortex has disappeared.



Streamlines in a piece of the superconducting FIG. 3. shell, for the same magnetic fields as in Fig. 2. The coordinates are the same as in Fig. 2, but now  $0 \le |\theta| \le 0.1\pi$ . In (a) and (b) we see streamlines through  $\theta = 0$  that carry electric current to the right (assuming that the magnetic field comes out of the page). These streamlines circulate around the superconducting loop (enclose the hollow region). At the right we see part of the screening currents, in clockwise circuits that do not enclose the hollow region. In (c) we see two counterclockwise streamlines around the quantum vortex, three streamlines around the loop and the screening currents at the right. Along a path around the vortex the phase of the order parameter changes by  $2\pi$ . In (d) the vortex has moved towards the inner boundary; the current around the loop has now become counterclockwise. As the magnetic field increases, the vortex moves down until it disappears and the counterclockwise current around the loop increases. The bottom frame shows a "panoramic" view of half of the shell,  $0 < |\theta| < \pi$ . The magnetic field is the same as in (d). The thick lines are streamlines and the thin lines are lines of constant  $|\psi|$ . On this scale,  $|\psi|$  looks independent of r and the currents around the vortex and around the loop do not show up.

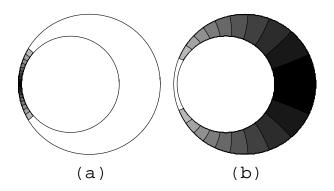


FIG. 4. Contour plot of  $|\psi|$  for a sample with cylindrical inner and outer boundary. Darker areas denote smaller values of  $|\psi|$ . For the chosen flux values,  $\psi = 0$  roughly in the middle of the darkest areas. (a)  $\Phi = 2.5713\Phi_0$ . (b)  $\Phi = 3.61\Phi_0$ . The flux range for the presence of the vortex in case (b) is about forty times larger than in case (a).